Journal of Electroanalytical Chemistry 738 (2015) 138–144

Contents lists available at ScienceDirect

Journal of Electroanalytical Chemistry

journal homepage: www.elsevier.com/locate/jelechem

A rapid, green and controllable method to fabricate the electrodeposition of a film of reduced graphene oxide as sensing materials for the determination of matrine

Liang Yan [a], Xiang Yu [b], Chunlei Zhao [b], Longwei Wang [b], Fei Wang [b,*]

[a] School of Civil Engineering and Communication, North China University of Water Resources and Electric Power, Zhengzhou 450045, China
[b] Department of Material and Chemistry Engineering, Henan Institute of Engineering, Zhengzhou 450007, China

ARTICLE INFO

Article history:
Received 16 September 2014
Received in revised form 3 November 2014
Accepted 5 November 2014
Available online 27 November 2014

Keywords:
Reduction of graphene oxide
Pulse potentiostatic method
Voltammetric sensor
Matrine

ABSTRACT

The electrodeposition of a film of reduced graphene oxide (ERGO) on a glassy carbon electrode (GCE) was achieved using pulse potential method (PPM) in the graphene oxide colloidal solution. For the first time, the electrodeposition of a film was applied to develop a high-sensitive electrochemical sensor for determination of matrine using linear sweep adsorptive stripping voltammetry (LSASV). Compared with bare GCE and ERGO film prepared by potentiostatic method (PM) modified electrode, the resulting electrodes (PP-ERGO/GCE) exhibited excellent response toward the oxidation of matrine by significantly enhancing the oxidation peak currents and decreasing the overpotential of matrine. Under the selected conditions, there exist the linear relation between the oxidation peak currents and matrine concentration in the range of 2.0×10^{-6}–1.2×10^{-4} mol L^{-1}, with detection limit of 5.0×10^{-7} mol L^{-1}. At the same time, the method can be successfully applied to the quantitative determination of matrine in injection and its result is satisfactory.

1. Introduction

Matrine, a typical quinolizidine alkaloid, is a main active ingredient of kinds of Sophora plants in traditional Chinese herbal drug. It has been extensively used in China for the treatment of viral hepatitis, cancer, cardiac and skin diseases [1–4]. Accordingly, accurate analytical method for matrine is necessary and some determination techniques have been developed, such as high performance liquid chromatography (HPLC) [5–8], liquid chromatography – mass spectrometer (LC-MS) [9–11], capillary electrophoresis (CE) [12] and chemiluminescence (CL) [13]. However, some of them are time-consuming and expensive or involve a tedious extraction process before detection. In contrast, electrochemical method is simple, rapid, sensitive and inexpensive. Furthermore, the redox properties of drugs can provide insight into their metabolic fate, their redox processes in vivo, and their pharmacological activity. Recently, some effort has been made to design the electrochemical sensor of matrine [14,15], but very limited.

Graphene, a perfect two-dimensional carbon material found in 2004 [16,17], is an ideal electrochemical material because of its very large 2D electrical conductivity [18], large surface area and low cost. Hence graphene-based modified electrodes, which can be prepared by various methods, have been explored as electrochemical sensors platforms [19–23]. Among these methods, the way of direct electrodeposition of reduced graphene oxide (ERGO) on glassy carbon electrode (GCE) has attracted considerable interest because it is simple, rapid, green and efficient [24–27]. Recently, it has been widely used in analytical [28–32] and industrial electrochemistry [33,34]. The electrochemical methods, such as cyclic voltammetry (CV) [28–31] and potentiostatic method (PM) [32–34], have been used. As we know, the pulse potential method (PPM) [35] is rarely applied in preparing the ERGO.

In this work, the ERGO film was directly achieved on GCE using PPM in the graphene oxide colloidal solution. The ERGO film were characterized by electrochemical methods and scanning electron microscopy. For the first time, the electrodeposition of a film was applied to develop a high-sensitive electrochemical sensor for determination of matrine using linear sweep adsorptive stripping voltammetry (LSASV). Electrochemical behaviors of matrine at the modified electrode were investigated by cyclic voltammetry (CV) and chronocoulometry (CC). At the same time, the method can be successfully applied to the quantitative determination of matrine in injection and its result is satisfactory.

* Corresponding author.
E-mail address: wf2003@zzu.edu.cn (F. Wang).

http://dx.doi.org/10.1016/j.jelechem.2014.11.006
1572-6657/

2. Experimental

2.1. Apparatus and Reagents

Model CHI 650A electrochemical system (CHI Instrumental, Shanghai, China) and RST5000 electrochemical workstation (Zhengzhou Shiruisi Instrument Co., Ltd., Zhengzhou, China) were employed for electrochemical techniques. Scanning electron microscopy (SEM) images were obtained with a Quanta 250 scanning electron microscope (FEI Company, Czech). Atomic Force Microscopy (AFM) images were obtained with a BenYuan CSPM-5500 atomic force microscopy (Guangzhou BenYuan nanometer Instrument Co., Ltd., Guangzhou, China). A standard three-electrode electrochemical cell was used with GCE (d = 3 mm) or modified GCE as a working electrode, platinum (Pt) wire as an auxiliary electrode and a saturated calomel electrode (SCE) as a reference electrode (the internal solution was saturated KCl solution). All the pH measurements were made with a PHS-3C precision pH meter (Leici Devices Factory of Shanghai, China), which was calibrated with standard buffer solution at 25 ± 0.1 °C every day.

Matrine was purchased from Aladdin Chemistry Co., Ltd (Shanghai, China). Stock solution (5.0×10^{-2} mol L^{-1}) of matrine was prepared with doubly distilled water and stored at 4 °C in the dark. Matrine injection was purchased from Jilin Yuhuang Pharma. Co., Ltd (Jilin, China). Graphite was purchased from Nanjing Xfnano Materials Tech Co., Ltd (Nanjing, China). All reagents were of analytical grade and were used as received. Double distilled water was used for all preparations.

2.2. Preparation of the modified electrode

Prior to modification, the bare GCE was polished successively with 0.3 and 0.05 μm Al_2O_3 powder and rinsed thoroughly with doubly distilled water between each polishing step. After that, the GCE was sonicated in ethanol and doubly distilled water each for 2 min, and dried under N_2 blowing. After that, the cleaned GCE was immersed in phosphate buffer solutions (PBS, pH 5.0) containing 0.85 mg mL^{-1} GO, and electrodeposited the GO by PPM under constant stirring. Graphene oxide (GO) was synthesized from graphite by the modified Hummers method [36]. The optimal parameters of electrodeposition were listed as follows: upper limit potential E_a, 0.1 V; lower limit potential E_c, −1.2 V; anodic pulse duration t_a, 0.6 s; cathodic pulse duration t_c, 0.3 s; experimental time t_{exp}, 150 s. The overall reduction time (t_{re}) can be calculated from the following equation: $t_{re} = t_{exp} \times t_c/(t_c + t_a)$. The obtained electrode was denoted as PP-ERGO/GCE. For comparison, the ERGO/GCE was also fabricated with the similar procedure by the PM. The reduction time of two methods is exactly the same.

3. Results and discussion

3.1. Morphologic characterization of the GO

The structure and morphology of the resulting GO deposited on the mica were characterized by AFM. The results showed that the GO sheets were almost single-layer, seen in Fig. 1. And the average thickness of single-layer GO sheets was about 1 nm.

3.2. Pulsed potentiostatic electrodeposition of RGO film on GCE

As applying a positive potential, GO sheets could be deposited on the electrode surface; because GO colloids exhibit negative charges in weak acid [37]. According to the literature [38], the as-deposited GO sheets can be electrochemically reduced at E = −1.1 V *vs.* SCE. Here we use the PPM to achieve the ERGO films, in which 0.1 V *vs.* SCE is used to deposit GO sheets on GCE, followed by applying −1.2 V *vs.* SCE to electrochemically reduce the as-deposited GO sheets to RGO sheets. The voltage profiles for the electrodeposition modes are schematically shown in the inset of Fig. 2.

To illustrate the pulse procedure used for the ERGO film, Fig. 2 shows the evolution in time of the E and i for the process of PPM. After the potential E_a is applied, the i increases sharply, reaching values close to zero. GO sheets were deposited on the electrode surface during the period. As potential E_c is imposed, the GO sheets close to the electrode surface start to react. The i drops sharply and then decreases tending to reach a steady value in potentiostatic mode. And then, when a new pulse starts, GO sheets could be diffused to areas where they have been quickly consumed while applying E_c. The distribution of GO sheets on the electrode surface is supposed to be more efficient and homogenous [39]. Therefore, the PPM can gain more uniform thin films.

3.3. Morphological characterization of ERGO film

To get more information on the successful preparation of ERGO films by PPM and illustrate the difference of electrochemical properties, morphologies of the ERGO/GCE (Fig. 3A) and PP-ERGO/GCE (Fig. 3B) were characterized using SEM. As showed in Fig. 3A, preparation of ERGO films by PM showed a loose, disorder and stacked surface. In contrast, preparation of ERGO films by PPM display closely associated with each other to form thin and crumpled sheets, and the edges of individual sheets were distinguishable with kinked and wrinkled areas, which is highly beneficial in maintaining a high surface area on the electrode and helpful in constructing an interface for the electrochemical sensors. Moreover, films barely show aggregation, indicating that the assembly of ERGO films by PPM on a solid substrate is a good way to achieve well-dispersed ERGO films and can prevent the aggregation.

3.4. Electrochemical characterization of PP-ERGO/GCE

The redox probe $[Fe(CN)_6]^{3-/4-}$ is sensitive to surface chemistry of carbon-based electrodes [40], and therefore was used to directly investigate the charge transfer property of the PP-ERGO/GCE. Fig. 4A shows the cyclic voltammograms (CVs) of bare GCE (curve a), ERGO/GCE (curve b) and PP-ERGO/GCE (curve c) in 1.0×10^{-3} mol L^{-1} $K_3[Fe(CN)_6]$ + 0.1 mol L^{-1} KCl solution. It proved the enhanced current response of the ERGO films toward $[Fe(CN)_6]^{3-/4-}$, indicating increased electrochemical active sites by ERGO surface modification. Moreover, the largest peak currents and the smallest ΔE_p of redox probe $[Fe(CN)_6]^{3-/4-}$ are observed on PP-ERGO/GCE, suggesting that the properties of the ERGO films prepared by PPM were superior to that of PM in increasing the active surface area of electrode and accelerating the electron transfer rate. Besides, Fig. 4B shows the influence of thickness of ERGO films on the peaks current of the redox probe. It is clear that the redox peaks current is directly proportional to the t_{re} (see the inset of Fig. 4B), indicating that PPM is an easily controllable and distinct advantage over CRGO methods.

At the same time, the average electroactive area of different electrode can obtain according to Randles–Sevcik formula [41]: $i_{pa} = 2.69 \times 10^5 n^{3/2} A D_o^{1/2} c_o v^{1/2}$, where i_{pa} refers to the anodic peak current (A); n is the electron transfer number; A is the surface area of the electrode (cm^2); D_o is the diffusion coefficient (cm^2 s^{-1}); c_o is the concentration of $K_3[Fe(CN)_6]$ (mol L^{-1}) and v is the scan rate (V s^{-1}). By exploring the redox peak current with scan rate, the average electroactive area of bare GCE, ERGO/GCE and PP-ERGO/GCE was calculated as 0.049, 0.080 and 0.139 cm^2, respectively. The results further indicated the preparation of the ERGO films

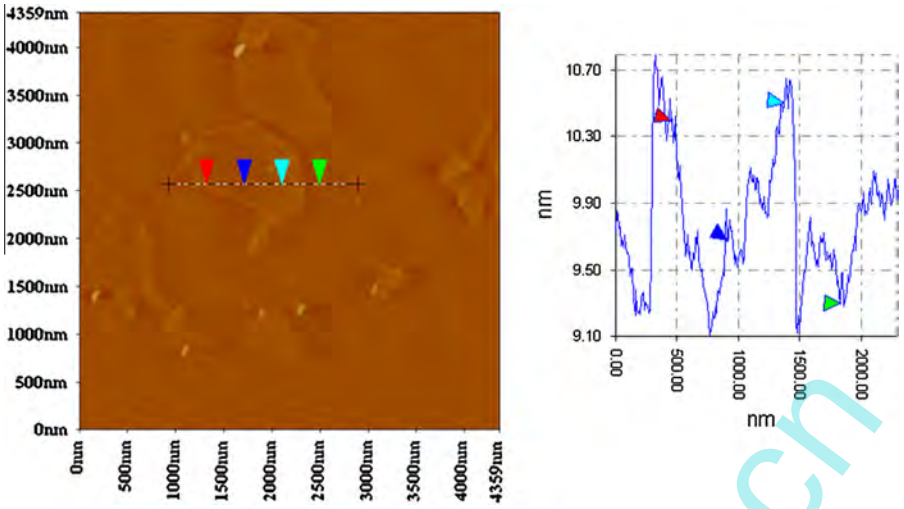

Fig. 1. AFM image of GO from its dilute aqueous dispersion on freshly cleaned mica.

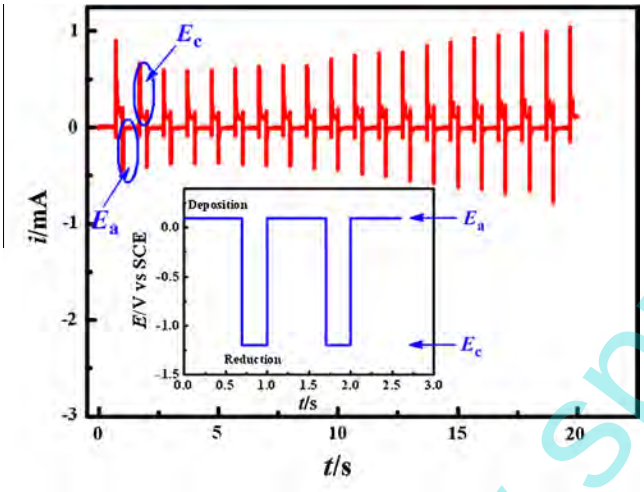

Fig. 2. Characteristic *i–t* response registered for pulsed electrodeposition; the inset in the figure outlines the *E–t* profile imposed during the electrodeposition of RGO films.

by PPM could further enhance the effective area of the electrode surface.

3.5. Voltammetric behavior of matrine at PP-ERGO/GCE

To highlight the particular feature of the proposed electrode, its voltammetric response was compared with another electrode. Fig. 5A displays CVs of 1.2×10^{-4} mol L^{-1} matrine in 0.2 mol L^{-1} PBS (pH 7.5) at bare GCE (curve a), ERGO/GCE (curve b) and PP-ERGO/GCE (curve c), respectively. As can be seen, matrine showed electrochemical activation on all electrodes. At bare GCE, the electrochemical response of matrine was very weak and only a very small bulge was observed at 1.02 V. In contrast, on the ERGO/GCE, the oxidation peak currents (i_{pa}) was increased significantly and the peak potentials (E_{pa}) was negatively shifted on about 0.771 V, indicating that the ERGO films could accelerate the electron transfer on the electrode surface to amplify the electrochemical signal due to its excellent electric conductivity and large specific surface area. When the PP-ERGO/GCE was applied, a distinct well-defined and more sensitive anodic peak appeared under the same experimental condition, of which the i_{pa} is about 33.2- and 6.4-fold higher than that of bare GCE and ERGO/GCE, respectively, and the E_{pa} is the lowest. The above results indicated that the ERGO films prepared by PPM can provide a more efficient interface and microenvironment for the electrochemical response of matrine.

For further highlighting the redox properties of matrine at PP-ERGO/GCE, successive CVs were performed. Fig. 5B shows CVs of the background (curve a) and successive CVs of 1.2×10^{-4} mol L^{-1} matrine in 0.2 mol L^{-1} PBS (pH 7.5) at PP-ERGO/GCE (curve b). It is clear that the anodic peak current decreased obviously in the second scan compared with that of the first one, and gradually reduced with successive cyclic sweep. The reason might be that the oxidation product of matrine adhered to the electrode surface and hindered the access of matrine. Besides, we also found that if the electrodes were kept in PBS (pH = 7.5) in the absence of matrine for 3 min under constant stirring, and then CV was carried out in the solution with scan potential window of between 0.0 V and 1.0 V (*vs.* SCE), until the peaks of matrine disappeared. Finally, the PP-ERGO/GCE surface will be restored to the initial state so that a new voltammogram then exhibits the same characteristics as those of the first cycle in Fig. 5B. Therefore, in the following discussion, the peak current is taken from the first cycle.

To further illustrate electrode reaction of matrine at PP-ERGO/GCE, the influence of potential scan rate (v) on i_{pa} of 1.2×10^{-4} mol L^{-1} matrine was studied by CV in different sweep rates from 50 to 300 mV s^{-1} (see Fig. 6). It is clear that the i_{pa} grow with the increasing of v and there are good linear relationships between log v and log i_{pa}. The dependence of i_{pa} on the v can be represented as $\log i_{pa} = -3.367 + 0.902 \log v$, $R = 0.999$. The slope of 0.902 proves that the oxidation process of matrine on the PP-ERGO/GCE is adsorption-controlled [42]. Furthermore, the E_{pa} shift positively with the increasing of v. According to Laviron's theory [43], for an irreversible anodic reaction, the relationship between E_{pa} and v is described as follows:

$$E_{pa}(V) = E^o - \frac{RT}{\alpha nF} \ln \frac{RTk_s}{\alpha nF} + \frac{RT}{\alpha nF} \ln v$$

where E^o is the formal standard potential; α is the charge transfer coefficient; k_s is the apparent electron transfer rate constant; and others have their usual meaning. The inserted calibration plot in Fig. 6 highlighted a linear relationship between the variation of E_{pa} with the ln v from 50 to 300 mV s^{-1} and a good linear equation was represented as E_{pa} (V) = 0.879 + 0.031 ln v (mV s^{-1}) (R = 0.999). From the slope of the straight line of E_{pa} against ln v, αn = 0.83 could be obtained. As for a totally irreversible electrode process, the value

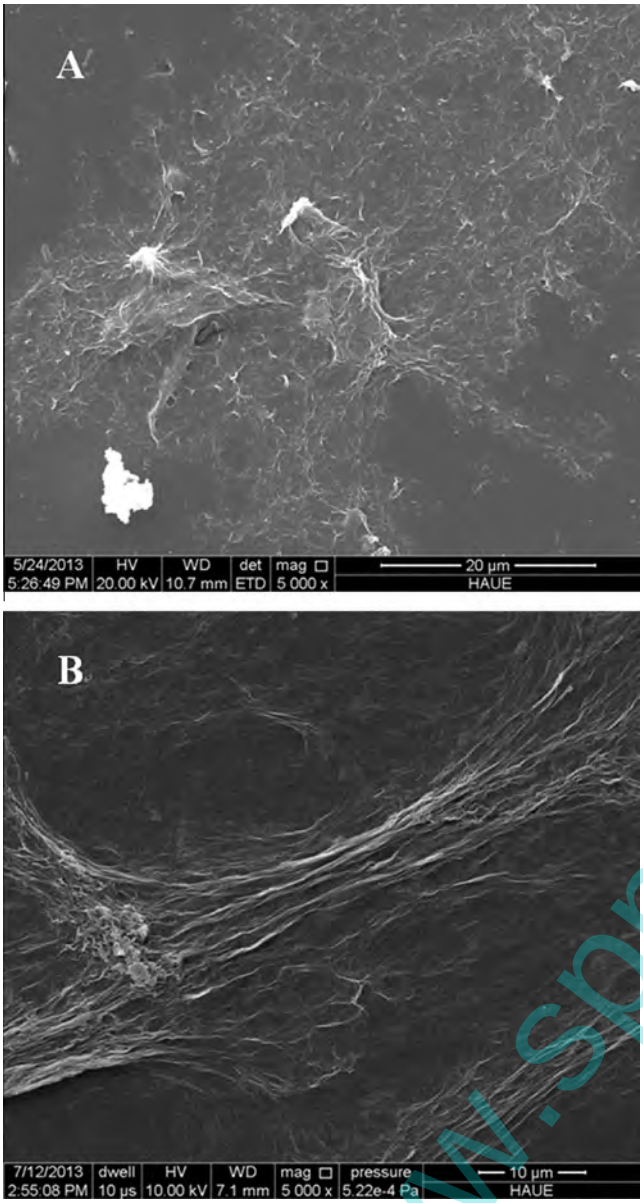

Fig. 3. The SEM images obtained from the ERGO/GCE (A) and PP-ERGO/GCE (B).

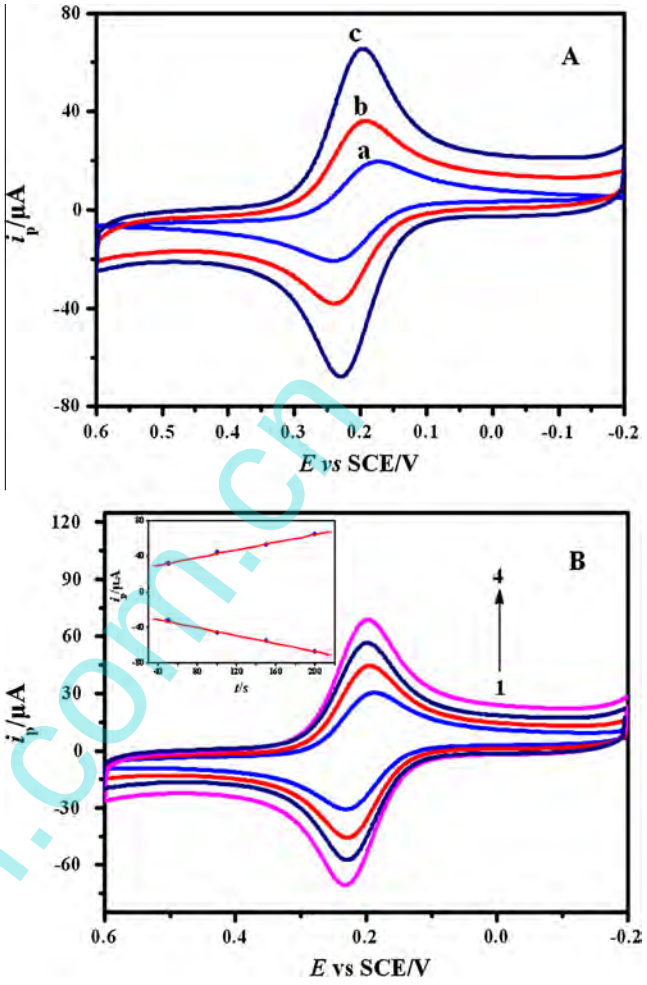

Fig. 4. (A) CVs of a bare GCE (curve a), ERGO/GCE (curve b) and PP-ERGO/GCE (curve c) in 1.0×10^{-3} mol L^{-1} $K_3[Fe(CN)_6]$ + 0.1 mol L^{-1} KCl solution, v = 0.05 V s^{-1}; (B) CVs of 1.0×10^{-3} mol L^{-1} $K_3[Fe(CN)_6]$ + 0.1 mol L^{-1} KCl solution on ERGO film prepared by PPM modified GCE under various t_{exp}, (1) t_{exp} = 50 s, (2) t_{exp} = 100 s, (3) t_{exp} = 150 s, (4) t_{exp} = 200 s; the inset is the dependence of oxidation peaks current on t_{exp}.

of α is assumed as 0.5 [43], thus, the value of n is calculated to be 2 as a reasonable conjecture. In return, α was 0.42. Meanwhile, value of k_s of 0.366 s^{-1} was calculated from the intercept of the straight line of E_{pa} *vs*. ln$v$. The value of E^o was determined to be 0.740 V from intercept of E_{pa} versus v plot on the ordinate by extrapolating the line to be v = 0.

3.6. Chronocoulometry investigations

For an adsorption driven electrode process, it is necessary to investigate its saturated absorption capacity (Γ_{max}) at the electrode surface. The chronocoulometry (CC) was used to perform this work in a blank solution (Fig. 7, curve a) and a 5.0×10^{-4} mol L^{-1} matrine solution (Fig. 7, curve b), respectively. The step potential from 0.0 V to 1.0 V was applied. The corresponding $Q \sim t^{1/2}$ plots were also performed and shown as inset in Fig. 7. According to the formula given by Anson [44]:

$$Q = \frac{2nFAc(Dt)^{1/2}}{\pi^{1/2}} + Q_{dl} + Q_{ads}$$

where Q_{dl} is the double-layer charge and Q_{ads} is the Faradaic charge due to the oxidation of adsorbed matrine. The inset in Fig. 7 shows the linearized plot for Q-$t^{1/2}$. The value of Q_{ads} was obtained by the difference of two intercepts of the plot of Q-$t^{1/2}$ for curves a and b. According to the equation: $Q_{ads} = nFA\Gamma_{max}$, a value of 1.41×10^{-8} mol cm^{-2} was obtained for Γ_{max}.

3.7. Analytical applications and methods validation

3.7.1. Influence of supporting electrolyte and pH

The types of supporting electrolytes played a key role in the voltammetric responses of matrine. Various buffers such as acetarte, borate, citrate, phosphate and Britton–Robinson buffer were used. The best results with excellent sensitivity and sharper response were obtained with phosphate buffer (PBS). Therefore, studies were made in PBS, whose pH is ranging from 5.0 to 8.5 at a target concentration of 1.0×10^{-4} mol L^{-1} matrine solution. The results showed that the E_{pa} shifted to lower values as the pH increased. The relationship between the E_{pa} and pH could be fitted into the regression equation: E_{pa} (V) = 1.212–0.054 pH (R = 0.998), whose slope indicates that the same amounts of electrons and protons took part in the electrode reaction. Therefore, the oxidation mechanism for matrine can be written as Scheme 1, which is in

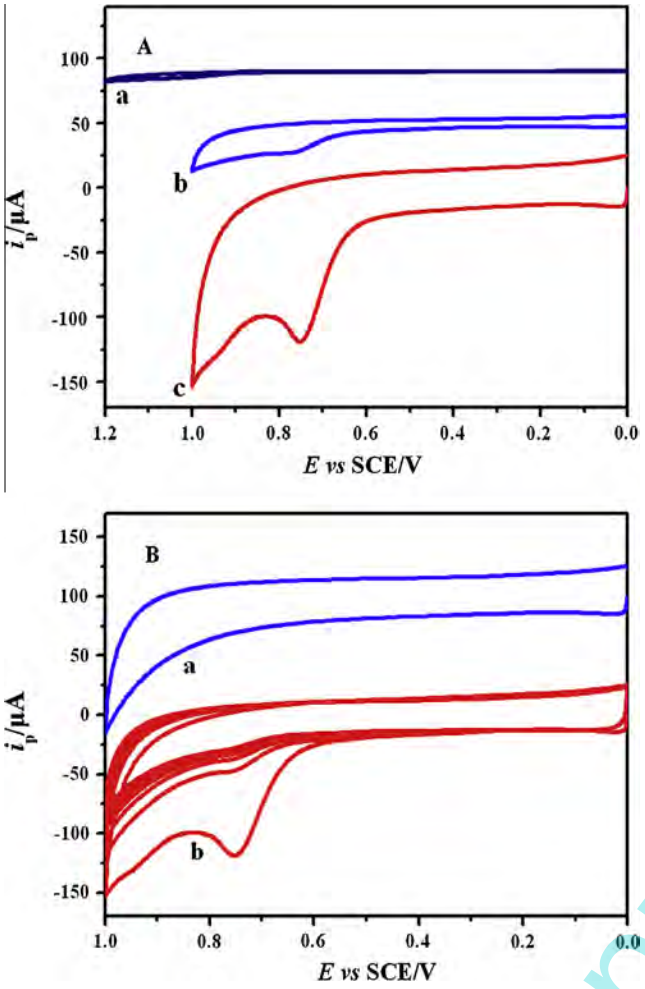

Fig. 5. (A) CVs of 1.2×10^{-4} mol L^{-1} matrine at a bare GCE (curve a), ERGO/GCE (curve b) and PP-ERGO/GCE (curve c) in 0.2 mol L^{-1} PBS (pH = 7.5), v = 0.05 V s^{-1}; (B) CVs of the background (curve a) and successive CVs of 1.2×10^{-4} mol L^{-1} matrine (curve b) at the PP-ERGO/GCE.

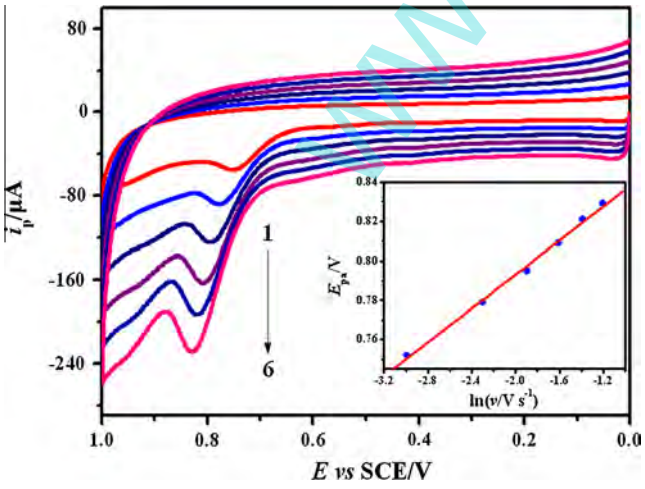

Fig. 6. CVs of 1.2×10^{-4} mol L^{-1} matrine at the PP-ERGO/GCE at different scan rate (from 1 to 6: 0.05, 0.10, 0.15, 0.20, 0.25, 0.30 V s^{-1}); the insets show the relationship of the peak potential E_{pa} against ln v.

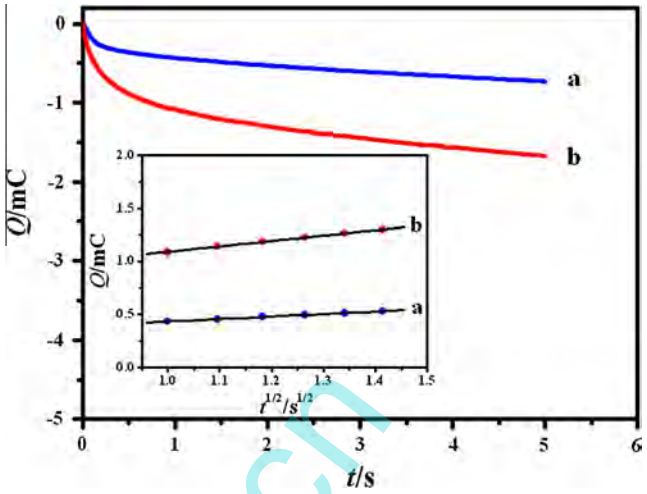

Fig. 7. Chronocoulometric curves of the background (curve a) and matrine (5.0×10^{-4} mol L^{-1}) (curve b) in 0.2 mol L^{-1} PBS (pH = 7.5) at the PP-ERGO/GCE; the inset is the corresponding $Q \sim t^{1/2}$ plots.

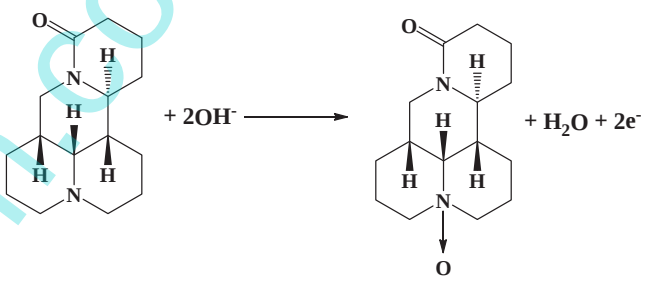

Scheme 1. Oxidation mechanism of matrine at PP-ERGO/GCE.

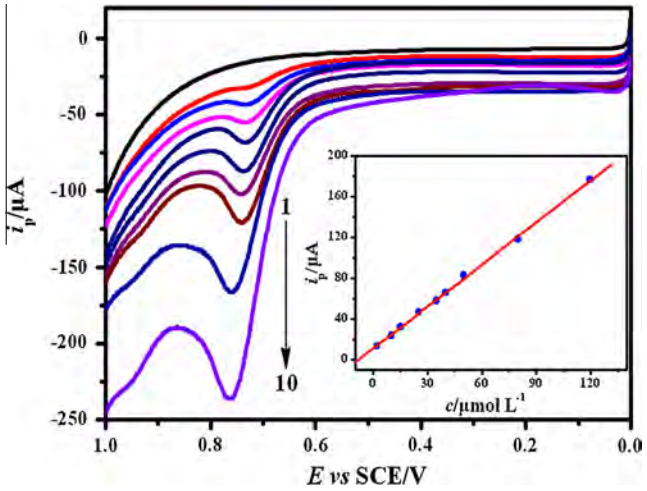

Fig. 8. Linear sweep adsorptive stripping voltammograms and their associated calibration plot (insert) for increasing concentrations of matrine at the PP-ERGO/GCE under optimum conditions; matrine concentration: (1) 0.0 mol L^{-1}, (2) 2.0×10^{-6} mol L^{-1}, (3) 1.0×10^{-5} mol L^{-1}, (4) 1.5×10^{-5} mol L^{-1}, (5) 2.5×10^{-5} - mol L^{-1}, (6) 3.5×10^{-5} mol L^{-1}, (7) 4.0×10^{-5} mol L^{-1}, (8) 5.0×10^{-5} mol L^{-1}, (9) 8.0×10^{-5} mol L^{-1}, (10) 1.2×10^{-4} mol L^{-1}.

Table 1
Comparison of determination of matrine by different methods reported.

Electrode	Methods	Linear range (mol L^{-1})	Detection limit (mol L^{-1})	Refs.
L-Cysteine/GO-Chitosan/GCE	SWASV	$4.0 \times 10^{-6} \sim 1.0 \times 10^{-4}$	2.0×10^{-6}	[14]
L-Cysteine/Au	CV	$2.0 \times 10^{-4} \sim 5.0 \times 10^{-3}$	–	[15]
PP-ERGO/GCE	LSASV	$2.0 \times 10^{-6} \sim 1.2 \times 10^{-4}$	5.0×10^{-7}	This work

SWASV: square wave anodic stripping voltammetry.
CV: cyclic voltammetry.
LSASV: linear sweep adsorptive stripping voltammetry.

Table 2
Determination results of matrine in injection samples by LSASV and UV.

LSASV (n = 5)						UV (n = 3)	
Declared content (mol L^{-1})	Amount found (mol L^{-1})	*RSD* (%)	Standard added (mol L^{-1})	Total found (mol L^{-1})	Recovery (%)	Amount found (mol L^{-1})	*RSD* (%)
4.00×10^{-2}	4.31×10^{-2}	2.9	2.00×10^{-2}	6.17×10^{-2}	93.0	4.40×10^{-2}	1.2

accordance with the report [14,15]. Besides, the i_{pa} vary very little in the range of 7.0–7.5; so solution pH of 7.5 were chosen in following experiments, which was close to human physiological pH.

3.7.2. Analytical conditions

In order to decrease the background current, LSASV was employed in the determination of matrine. Besides, to obtain a much more sensitive detection, 50 mV s^{-1} was chosen as a most suitable scan rate for the further experiments.

For an adsorbed-driven electrode reaction, it is good way for enhancing the detection sensitivity by preconcentration. In the experiments, the influence of the accumulation time (t_{acc}) on response currents of 5.0×10^{-7} mol L^{-1} matrine was estimated. The results showed that the i_{pa} increased greatly within 240 s and then enhanced slowly. For all we know, a longer t_{acc} will result in a better detection limit, but would also lead to a narrower linear range. For comprehensive consideration, 240 s was chosen as accumulation time. At the same time, the accumulation potential had little effect on the i_{pa}. So the accumulation was carried out under an open circuit.

3.7.3. Calibration curve, detection limit, stability, reproducibility and repeatability

Series concentrations of matrine standard solutions were detected under the optimized working conditions, as described above. Fig. 8 displayed the response of different concentration of matrine by LSASV. A linear relationship could be established between i_{pa} and the concentration of matrine in the range of $2.0 \times 10^{-6} \sim 1.2 \times 10^{-4}$ mol L^{-1}, seen the inset of Fig. 8. The linear regression equation and correlation coefficient are:

$$I_{pa} = 10.82 + 1.37c \ (R = 0.999)$$

where i_{pa} was the oxidation peak current in μA and c was the concentration of matrine in μmol L^{-1}. Standard deviations (SD) for the slope and intercept of the calibration curve were 0.00182 and 0.0997, respectively. Based on the signal-to-noise ratio of 3 (S/N) [45], the detection limit was obtained as 5.0×10^{-7} mol L^{-1}. These values confirmed the sensitivity of the proposed method for the determination of matrine.

The stability, reproducibility and repeatability of PP-ERGO/GCE are also estimated. It is seen that the modified electrode remain 93.7% of its initial current response to matrine after 14 days' storage, indicating the electrochemical sensor has the good stability. The reproducibility was examined from the response to 1.0×10^{-4} mol L^{-1} matrine at five modified electrodes prepared in the same conditions and a relative standard deviation (RSD) of 4.3% was obtained. The RSD of the response to 1.0×10^{-4} mol L^{-1} matrine was 4.1% for 5 successive measurements, indicating the electrochemical sensor has the good repeatability. All these observations indicate that PP-ERGO/GCE exhibit excellent stability, reproducibility and repeatability for detection of matrine.

The proposed PP-ERGO/GCE for matrine determination was compared with other reported method and the results were showed in Table 1. It is obvious that the proposed electrodes can achieve wider linear concentration ranges and lower detection limits. Besides, this research suggests that the preparation of ERGO film by PPM as voltammetric sensors might be a very promising direction in trace analysis of electrochemistry.

3.7.4. Interference studies

The influence of various potentially interfering substances for determination of 1.0×10^{-4} mol L^{-1} matrine was studied by LSV. The results indicated that 100-fold of Ca^{2+}, Zn^{2+}, Cu^{2+}, Cl^{-}, SO_4^{2-}, NO_3^{-}, Ac^{-}, glucose, sucrose and amylum, 10-fold of hypoxanthine, glycine, glutamic acid, ascorbic acid, uric acid, epinephrine, adenine had almost no influence on the determination and the tolerance limit was estimated to be less than 5% of the relative error, indicating the present method was adequate for the determination of matrine in real samples.

3.8. Determination of matrine in injection samples

In order to evaluate the validity of the proposed method, it was employed to determine matrine in injection samples. The sample was diluted with the supporting electrolyte to operate in the linear range of the method and to reduce the matrix effect. After the content of matrine was evaluated, a standard matrine solution was added into the sample and the total content of matrine was determined to calculate the recovery (see Table 2). For testing the accuracy of the proposed method, the same sample was analyzed using UV–vis method and the result was listed in Table 2 too. The contents obtained from the proposed method and UV–vis method were compared using *t*-test under 95% confidence levels. The results showed no significant difference between them. The results showed that the method was reliable for the quantitative determination of matrine in injection samples.

4. Conclusions

We have demonstrated PPM to prepare ERGO films for the sensitive detection of matrine. The ERGO films at the modified electrode exhibited excellent response toward the oxidation of

matrine by significantly enhancing the oxidation peak currents and decreasing the overpotential of matrine, superior to that of potentiostatic method. Wide linear concentration ranges, low detection limits, and excellent reproducibility and stability were made on the modified electrode, indicating the ERGO films prepared by PPM might be a very promising platform for analytical sensing.

Conflict of interest

There is no conflict of interest.

Acknowledgements

We gratefully acknowledge the financial support by the Joint Funds of the National Science Foundation of China – Henan Province People's Government (No. U1304213) and the funding Program for Young Key Teachers in Universities of Henan Province (No. 2013GGJS-183).

References

[1] L.F. Guo, S.S. Tong, J.N. Yu, X.M. Xu, China J. Chin. Mater. Med. 38 (2013) 3409–3412.
[2] L.H. Zhang, B.E. Chen, M.J. Pan, Chin. Tradit. Herb. Drugs 40 (2009) 1000–1003.
[3] M. Liu, X.Y. Liu, J.F. zheng, China J. Chin. Mater. Med. 28 (2003) 801–804.
[4] K.L. Miao, J.Z. Zhang, Y. Dong, Y.F. Xi, Nat. Prod. Res. Dev. 13 (2001) 69–73.
[5] Z. Yin, S. Ma, J. Wang, X. Shang, J. Anal. Meth. Chem. 2013 (2013) 1–5.
[6] X. Yang, B.L. Guo, H.Y. Hu, W.H. Huang, H.P. Qiao, S.C. Fan, Z.G. Guan, China J. Chin. Mater. Med. 38 (2013) 2844–2847.
[7] W. Liu, Z. Ruan, M. Bai, China J. Chin. Mater. Med. 35 (2010) 1818–1819.
[8] Y.A. Jung, X. Wan, H. Yan, K.H. Row, J. Liq. Chromatogr. Rel. Technol. 31 (2008) 2752–2761.
[9] X. Liu, Y. Tian, F. Dong, J. Xu, Y. Li, X. Liang, Y. Wang, Y. Zheng, J. AOAC Int. 97 (2014) 218–224.
[10] F. Yang, D.P. Zhen, Z.C. Liu, Y.H. Lin, J. Chen, S.P. Chen, G.N. Chen, Chin. J. Anal. Chem. 39 (2011) 556–559.
[11] X.L. Zhang, H.R. Xu, W.L. Chen, N.N. Chu, X.N. Li, G.Y. Liu, C. Yu, J. Chromatogr. B 877 (2009) 3253–3256.
[12] Y.R. Ku, L.Y. Chang, J.H. Lin, L.K. Ho, J. Pharm. Biomed. Anal. 28 (2002) 1005–1010.
[13] J. You, J. Liu, D. Chen, Z. Song, J. Anal. Chem. 69 (2014) 17–21.
[14] F. Zhao, L. Wang, Y. Liu, G. Song, F. Wang, B. Ye, Electroanalysis 24 (2012) 691–698.
[15] Y. Miao, J. Chen, X. Wu, Surf. Rev. Lett. 15 (2008) 537–543.
[16] A.K. Geim, Science 324 (2009) 1530–1534.
[17] A.K. Geim, K.S. Novoselov, Nat. Mater. 6 (2007) 183–191.
[18] J.L. Zhang, H.J. Yang, G.X. Shen, P. Cheng, J.Y. Zhang, S.W. Guo, Chem. Commun. 46 (2010) 1112–1114.
[19] L. Chen, Y. Tang, K. Wang, C. Liu, S. Luo, Electrochem. Commun. 13 (2011) 133–137.
[20] C.X. Lim, H.Y. Hoh, P.K. Ang, K.P. Loh, Anal. Chem. 82 (2010) 7387–7393.
[21] Y.R. Kim, S. Bong, Y.J. Kang, Y. Yang, R.K. Mahajan, J.S. Kim, H. Kim, Biosens. Bioelectron. 25 (2010) 2366–2369.
[22] M. Zhou, Y. Zhai, S. Dong, Anal. Chem. 81 (2009) 5603–5613.
[23] N.G. Shang, P. Papakonstantinou, M. McMullan, M. Chu, A. Stamboulis, A. Potenza, S.S. Dhesi, H. Marchetto, Adv. Funct. Mater. 18 (2008) 3506–3514.
[24] H.L. Guo, X.F. Wang, Q.Y. Qian, F.B. Wang, X.H. Xia, ACS Nano 3 (2009) 2653–2659.
[25] Y. Shao, J. Wang, M. Engelhard, C. Wang, Y. Lin, J. Mater. Chem. 20 (2010) 743–748.
[26] J.F. Ping, Y.X. Wang, K. Fan, J. Wu, Y.B. Ying, Biosens. Bioelectron. 28 (2011) 204–209.
[27] Z.J. Wang, X.Z. Zhou, J. Zhang, F. Boey, H. Zhang, J. Phys. Chem. C 113 (2009) 14071–14075.
[28] Z.L. Feng, Y.Y. Yao, J.K. Xu, L. Zhang, Z.F. Wang, Y.P. Wen, Chin. Chem. Lett. 25 (2014) 511–516.
[29] L. Ding, Y.P. Liu, J.P. Zhai, A.M. Bond, J. Zhang, Electroanalysis 26 (2014) 121–128.
[30] Y. Liu, H. Zhao, X. Qingji, S. Lingen, G. Tiean, L. Zou, B. Lijuan, Y. Shouzhuo, T. Xinman, L. Xubiao, L. Shenglian, Sens. Actuat. B 188 (2013) 894–901.
[31] C. Fei, Z. Xiaoli, J. Solid State Electrochem. 17 (2013) 167–173.
[32] L. Gaonan, L. Tongtong, D. Ying, C. Yong, S. Fan, S. Wei, S. Zhenfan, J. Solid State Electrochem. 17 (2013) 2333–2340.
[33] T.T. Liu, G.J. Shao, M.T. Ji, Mater. Lett. 122 (2014) 273–276.
[34] Y.C. Eeu, H.N. Lim, Y.S. Lim, S.A. Zakarya, N.M. Huang, J. Nanomater. 2013 (2013) 1–6.
[35] A. Davies, P. Audette, B. Farrow, F. Hassan, Z.W. Chen, J.Y. Choi, A.P. Yu, J. Phys. Chem. C 115 (2011) 17612–17620.
[36] W.S. Hummers, R.E. Offeman, J. Am. Chem. Soc. 80 (1958). 1339-1339.
[37] S. Park, J. An, R.D. Piner, I. Jung, D. Yang, A. Velamakanni, S.T. Nguyen, R.S. Ruoff, Chem. Mater. 20 (2008) 6592–6594.
[38] L.Y. Chen, Y.H. Tang, K. Wang, C.B. Liu, S.L. Luo, Electrochem. Commun. 13 (2011) 133–137.
[39] M.S. Chandrasekar, M. Pushpavanam, Electrochim. Acta 53 (2008) 3313–3322.
[40] P.H. Chen, M.A. Fryling, R.L. McCreery, Anal. Chem. 67 (1995) 3115–3122.
[41] A.J. Bard, L.R. Faulkner, Electrochemical Methods, Fundamentals and Applications, 2nd ed., Wiley, New York, 2001.
[42] Y.F. Li, K.J. Li, G. Song, J. Liu, K. Zhang, B.X. Ye, Sens. Actuators B 182 (2013) 401–407.
[43] E. Laviron, J. Electroanal. Chem. 101 (1979) 19–28.
[44] F.C. Anson, Anal. Chem. 36 (1964) 932–934.
[45] J.N. Miller, J.C. Miller, Statistics and Chemometrics for Analytical Chemistry, fourth ed., Pearson Education Limited, London, 2000.